Aspect Ratio Dependence of the Enhanced Fluorescence Intensity of Gold Nanorods: Experimental and Simulation Study

Susie Eustis and Mostafa El-Sayed*

Laser Dynamics Laboratory, School of Chemistry and Biochemistry, Georgia Institute of Technology, Atlanta, Georgia 30332

Received: June 2, 2005; In Final Form: June 28, 2005

Experimental observations and theoretical treatments are carried out for the band shape and relative intensity of the emission from gold nanorods of various aspect ratios in the range between 2.25 (1.5 theory) and 6.0 (9 theory). The calculation of the fluorescence spectra requires knowledge of the nanorod size distribution, the enhancement factors, and the shape of the unenhanced fluorescence spectrum. The size distribution is determined from the fit of the observed absorption spectrum for each value of aspect ratio studied to the theoretical model of Gans. The theory by Boyd and Shen is used for calculating the enhancement of the fluorescence spectrum of the previously observed weak emission of bulk gold, which originates from the interband transition. This is carried out for nanorods of different aspect ratios. To compare theory to the observed nanorod fluorescence spectra, which suffer from self-absorption, the calculated nanorod fluorescence spectra are corrected for this effect using the observed absorption spectra. The comparison between the observed and the calculated fluorescence band shapes is found to be good. The calculated changes in the relative intensities upon changing the aspect ratios are found to be much greater than that observed. This is due to the fact that for the observed emission of all the nanorods studied nonradiative processes dominate the relaxation mechanism of the excited state, a fact that was not included in the theoretical treatments.

Introduction

The optical properties of noble metal nanoparticles are of great interest due to the strong surface plasmon resonance absorption in the visible region of the electromagnetic spectrum.[1,2] This strong absorption leads to the enhancement in the electromagnetic field near the surface, leading to enhancement of Raman and Rayleigh scattering processes. Gold nanorods have two plasmon resonance absorptions, one due to the transverse oscillation of electrons around 520 nm regardless of the aspect ratio. The other absorption is due to the longitudinal oscillation of the electrons, which depends on the aspect ratio of the nanorod. The resonances are due to a collective oscillation of the free electrons through the metal, which depend on the boundary conditions.

Bulk gold fluorescence, first observed by Mooradian in 1969,[3] is very weak with a quantum yield of 10^{-10}. Recent research has produced a number of reports of fluorescence enhancement in nanoparticles[4−17] as well as a background emission believed to be fluorescence in surface-enhanced Raman spectroscopy (SERS).[18−23] Gold nanoclusters fluoresce in the visible and near-IR with quantum yields[4−8,15] of up to 10^{-3}. Emission from gold clusters was first observed[4] in 1998 by Wilcoxon et al. where small gold clusters were found to fluoresce with quantum efficiencies in the $10^{-4}-10^{-5}$ range. Recently, emission from a single species of gold clusters has been identified.[7−9] The emission wavelength changes with the size of the cluster, with Au_8 emitting light below 500 nm[8] and Au_{28} emitting light above 800 nm.[7] Blinking has also been observed in single-molecule studies in both gold and silver on the second time scale.[11,16]

Experimental and theoretical results published by Shen and Boyd[24−26] ascribe the emission of noble metals to the band structure of the metal. Large enhancement in emission on roughened metal surfaces was attributed to local enhancement in the field around the surface of the metal. This same enhancement is observed in SERS activity.[27] The emission is attributed to a recombination between the electrons and holes in the interband recombination.

Previous studies[14,17] of this group were able to use a theoretical model to place an upper boundary on the lifetime of the fluorescence emission from gold nanorods as a function of the aspect ratio. Large enhancement in fluorescence emission was found for electrochemically synthesized rods over spheres with quantum yields of $10^{-4}-10^{-5}$. Experimentally, the emission wavelength increased linearly with the aspect ratio, and the enhancement factor was found to increase linearly with the square of the aspect ratio.[17] Theoretically, the enhancement of the emission from nanorods was modeled using a lighting rod effect to account for the enhancement of the electric field near the surface of the nanorods.[14,17] The upper bound on the lifetime was determined to be 50 fs and is likely related to the dynamics of the holes created in the d-bands immediately after irradiation.[14]

This paper presents an expansion of previous research looking at high aspect ratio nanorods made by a new synthesis technique and extending the theoretical model. This paper shows that at higher aspect ratios the enhancement decreases and broadens due to the diminishing coupling between the longitudinal plasmon resonance oscillation and the interband transition and the size distribution. Emission is not observed at the wavelengths predicted in the previous theoretical model[17] due to the importance of the emission of bulk gold. The difference in intensity changes between experimental and theoretical emission spectra are due to the importance of nonradiative transitions.

Experimental Methods

The gold nanorods were prepared by a slightly modified technique as described previously by this group.[28] Briefly, a

* Author to whom correspondence should be addressed. E-mail: mostafa.el-sayed@chemistry.gatech.edu.

10.1021/jp052951a CCC: $30.25
Published on Web 08/09/2005

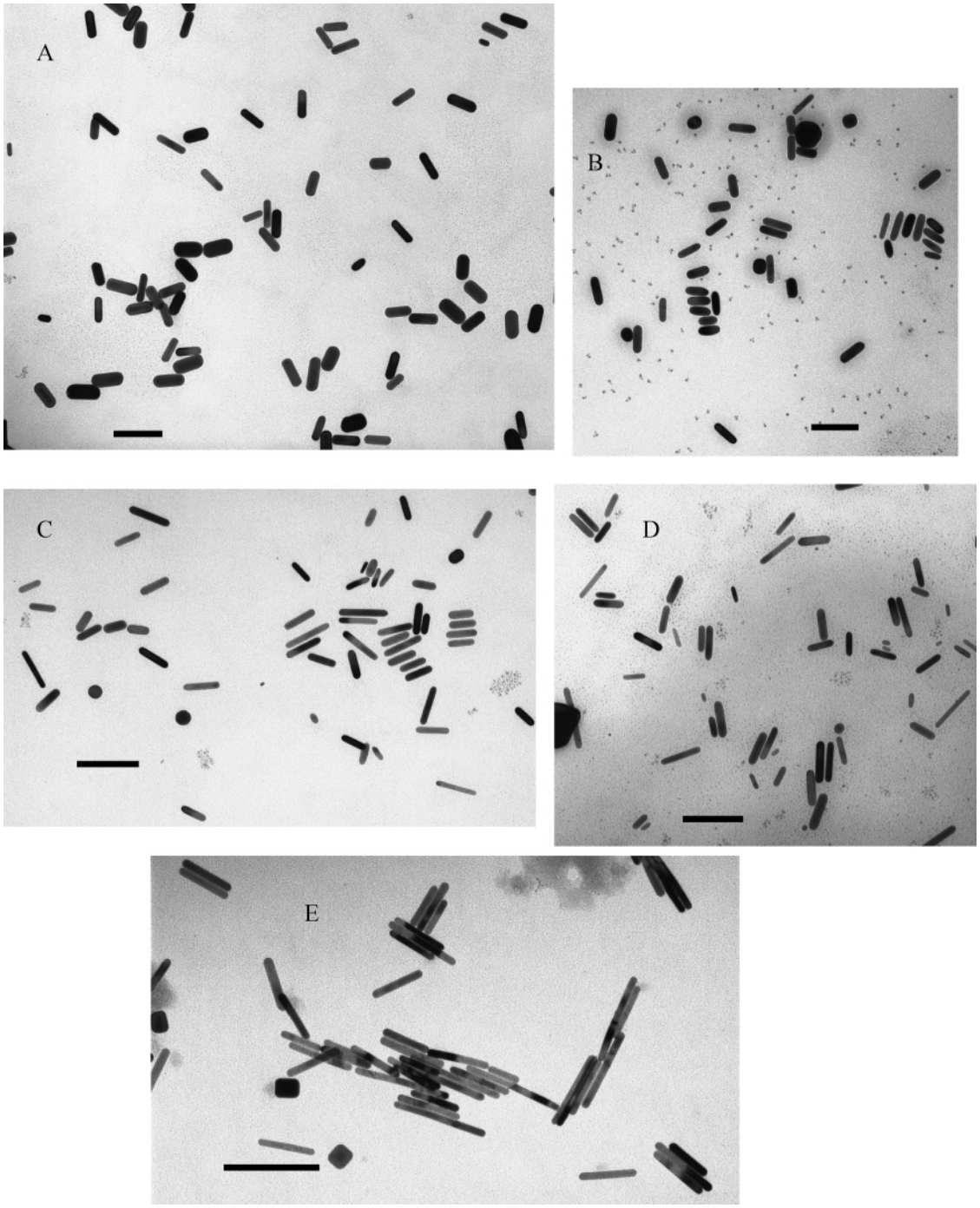

Figure 1. TEM images of gold nanorods used in fluorescence studies: (A) Au630, (B) Au700, (C) Au850, (D) Au900, and (E) Au1000. All scale bars represent 100 nm. Aspect ratios are given in Table 1.

seed solution is generated by adding ice-cold $NaBH_4$ to a solution of $HAuCl_4$ and hexadecyltrimethylammonium bromide (CTAB). The solution was kept at 25 °C for a few minutes before use. A brownish yellow color was observed in all seed solutions used. The growth solution contained 5 mL of a solution of 0.20 m CTAB and 0.25 m benzyldimethylammonioum chloride hydrate (BDAC), which is added to 0.20 mL of 4.0 mM $AgNO_3$. Then, 5.0 mL of 0.90 mM of $HAuCl_4$ is added and 54 μL of 0.10 M ascorbic acid. Twelve microliters of seed solution is then added to the solution, which is left undisturbed for 4 h for the nanorods to grow. Kinetic growth conditions determine the aspect ratio of the nanorods generated, with narrower widths in the higher aspect ratio samples.

The optical absorbance spectra were recorded on a Shimadzu UV-3101-PC UV−vis−near-IR scanning spectrometer. Fluorescence measurements were taken on a PTI model C60 steady-state spectrometer. Average volume was determined from TEM images using 100 kV on a JEOL100 transmission electron microscope (TEM) using Image Pro Plus, version 4.5, to determine the length and width of the nanorods. Models of absorption spectra using equations presented below are used to determine the aspect ratio distribution for the calculations of the fluorescence emission due to the bulk average represented in the absorption and emission spectra.

Experimental Results

Figure 1 shows TEM images of gold nanorod samples used in this paper. The samples are cataloged in Table 1 with the maximum longitudinal plasmon resonance and aspect ratio given for each sample. Due to the kinetic growth used to generate

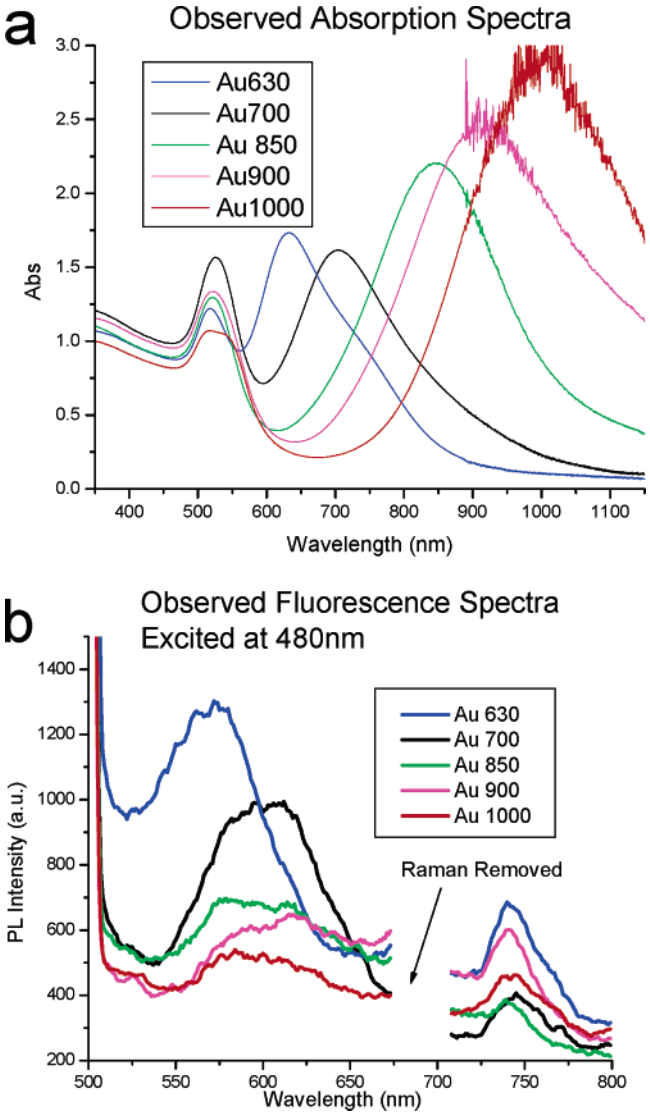

Figure 2. (a) Absorption spectra of gold nanorods shown in Figure 1. (b) Fluorescence spectra of gold nanorods shown in Figure 1 upon 480-nm excitation.

these samples, both the length and the width change as the aspect ratio is increased.

Figure 2a shows the optical absorption of the samples used in this experiment. The optical absorption spectra in Figure 2a exhibit the same behavior Link et al.[29−31] described theoretically where as the aspect ratio of the nanorod increases the longitudinal plasmon resonance increases in wavelength and intensity for a given concentration of nanorods. Figure 2b shows the fluorescence emission from the gold nanorods after excitation with 480-nm light. As the average aspect ratio increases from 2.25 to 3.25, the emission red-shifts from 575 to 600 nm. At higher aspect ratios, the emission remains centered around 600 nm but decreases in intensity. The fluorescence shown in Figure 2b are similar to the previous emission spectra observed for gold nanorods.[17] The growth methods for the two studies are different, chemical versus electrochemical reduction, using different surfactants to stabilize the surface of the gold nanorod during growth. Furthermore, the electrochemical method produces rods having single crystals. The seed growth method generates nanorods with more defects as the aspect ratio increases. By observation of the similarity between the observed fluorescence, it can be said that the fluorescence is due to the gold nanorods in solution and is not affected by differing surfactants.

Figure 3 presents the emission spectrum for sample Au630 after excitation with 407−437-nm light. Raman bands are easily identified; besides being relatively sharp, they shift with changing the excitation wavelength. The fluorescence band maxima do not change with changing the excitation wavelength. Thus, in Figure 3, the emission bands at 575 and 730 nm remain constant, while a Raman band is observed shifting from 585 to 625 nm upon changing the excitation wavelength from 407 to 437 nm. The inset further confirms this analysis by converting the *x*-axis to Δ wavenumbers. The Raman scattering is observed at a constant shift of 7000 cm^{-1} from the incident wavelength. This energy is improbable to correspond to any molecular vibration and could be due to an electronic transition.

The quantum yield of these nanorods was measured relative to rhodamine 6G (0.9) and is found to be on the order of 10^{-4}. This suggests that the nanorods have an observed lifetime that is 10^{-4} times smaller that that of rhodamine 6G, which is $\sim 10^{-9}$ s, i.e., $\sim 10^{-9}$ s $\times$ 10^{-4} $\approx$ 10^{-13} s. This is consistent with a previous attempt[14] to measure the nanorod lifetime, which was found to be less than 50 fs. This suggests that the observed nanorod fluorescence lifetime is dominated by rapid (<50 fs) nonradiative processes and does not measure the radiative lifetime of the emission.

Theoretical Calculation

To simulate the fluorescence emission of the gold nanorod samples presented here, the absorption spectrum is modeled to obtain aspect ratio distributions. The aspect ratio distributions determined from TEM results did not give as good agreement with the observed emission due to the limited statistics (~200 nanorods per sample) and the change of state of the nanoparticle environment (liquid to solid support) necessary for TEM analysis. The absorption spectra are a measure of the bulk solution properties, as are the fluorescence emission spectra. The emission is calculated by first calculating the enhancement factors for gold nanorods, often referred to as the "lightning rod effect" according to Shen and Boyd[24−26] as reported by Mohamed et al.[17] This enhancement factor is multiplied by the aspect ratio distribution determined from fitting the theoretical simulated absorption spectrum to the observed one, modeling the absorption spectrum to match the experimental samples. This enhancement factor is then multiplied by the emission of bulk gold measured by Mooradian[3] as suggested in the equations presented by Shen and Boyd.[24−26] When theoretical predictions for this emission[32] are used in place of experimental data, the emission at higher wavelengths is found to be overestimated and does not fit the observed spectra. For a closer agreement with experimental data, the self-absorption of the solution is taken into account by subtracting the experimental absorption spectra from the predicted emission spectra. The corrected band shapes of the different emission spectra simulated in this manner are found to be in good agreement with that observed. The details of these calculations are given below, and the results of these calculations are presented in Figure 4.

The absorption and emission of gold nanorods were calculated using a structure factor. Absorption spectra of gold nanorods have been modeled previously by Link et al.[29−31] They apply Gans'[33] extension of Mie's theory[34] to calculate the absorption spectra of gold nanorods of different aspect ratios and medium dielectric constants. The extinction coefficient, γ, can be

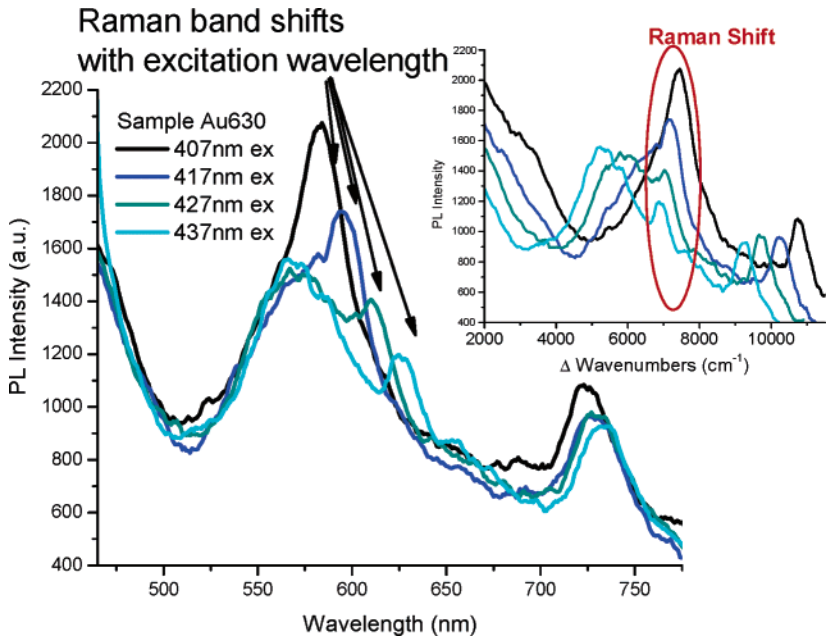

Figure 3. Emission spectra of sample Au630 with different excitation wavelengths. The inset shows the same data, with the *x*-axis converted to Δ wavenumbers.

calculated in the dipole approximation (which should hold for these samples) as follows.

$$\gamma = \frac{2\pi NV{\epsilon_m}^{3/2}}{3\lambda}\sum_J \frac{(1/{P_J}^2)\epsilon_2}{\left(\epsilon_1 + \frac{1-P_J}{P_J}\epsilon_m\right)^2 + {\epsilon_2}^2} \qquad (1)$$

where

$$P_A = \frac{1-e^2}{e^2}\left[\frac{1}{2e}\ln\left(\frac{1+e}{1-e}\right) - 1\right]$$

$$P_B = P_C = \frac{1-P_A}{2}$$

and

$$e = \sqrt{1-\left(\frac{b}{a}\right)^2}$$

P_A, P_B, and P_C are the shape factors as a function of e, which is a function of the inverse of the aspect ratio (a/b).

Boyd and Shen[24−26] have proposed a model for emission enhancement for gold nanorods. Their theory is based on a local-field factor $L(\omega)$, which is given by the dimensions of a hemispheroid of length a and width b (aspect ratio = a/b), and the dielectric constant of gold is obtained from Johnson and Christy.[35]

$$L(\omega) = L_{LR}\left[\frac{\epsilon(\omega)}{\epsilon_m} - 1 + L_{LR}\left(1 + \frac{i4\pi^2 V(1-\epsilon(\omega))\epsilon_m^{1/2}}{3\lambda^3}\right)\right]^{-1} \qquad (2)$$

where $L_{LR} = A^{-1}$

$$A = \left[1 - \frac{\xi Q_1'(\xi)}{Q_1(\xi)}\right]^{-1}$$

$$\xi = \left[1 - \left(\frac{b}{a}\right)^2\right]^{-1/2}$$

$$Q_1(\xi) = \left(\frac{\xi}{2}\right)\ln\left[\frac{\xi+1}{\xi-1}\right] - 1$$

$$Q_1'(\xi) = \frac{dQ_1(\xi)}{d\xi}$$

where λ is the wavelength, ϵ_m is the dielectric constant of the medium, and $V = (4/3)\pi a(b/2)^2$ is the volume of the nanorod. The emitted luminescence is given by

$$P_{1sph}(\omega, a/b, V) = \beta_1 2^4 |E_o|^2 V[L^2(\omega_1)L^2(\omega_2)] \qquad (3)$$

where $L^2(\omega_1)$ is the local-field factor at the excitation wavelength and $L^2(\omega_2)$ is the local-field factor at the emission wavelength, $|E_o|^2$ is the incident electric field, and β_1 is a proportionality constant including the intrinsic luminescence spectrum of gold. The average volume of sample nanorods (as determined from TEM) was used for all of the calculations of the emission enhancement.

To first calculate the absorption spectrum of the samples, A given by Boyd and Shen[24−26] was used in place of P_J as the shape factor. Thus, the transverse plasmon is not calculated, and eq 1 can be simplified to the following equation

$$\gamma = \frac{2\pi NV{\epsilon_m}^{3/2}}{3\lambda}\frac{(\epsilon_2/A^2)}{\left(\epsilon_1 + \frac{1-A}{A}\epsilon_m\right)^2 + {\epsilon_2}^2} \qquad (4)$$

This equation is calculated for various different aspect ratios between 1.5 and 9, every 0.25. Then, an aspect ratio distribution is multiplied by the different curves, and the sum is fitted to the longitudinal plasmon resonance absorption by adjusting the distribution to match the experimental observed absorption spectra, where ϵ_m is 1.77 for all samples. The absorption spectra calculated are presented in Figure 4a. This aspect ratio distribu-

tion and $\epsilon_m = 1.77$ are used in the eq 2, for the fluorescence enhancement of the samples. (It should be noted that the simple linear equation to predict ϵ_m presented by Link et al.[29−31] is not valid for higher aspect ratio nanorods, due to the deviation from linearity in $\epsilon(\omega)$ above 800 nm.)

Mohamed et al.[17] previously reported the calculated results of $|L(\omega_1)^2 L(\omega_2)^2|$ as a function of aspect ratio as given by eq 3. The results from this equation for the enhancement of gold nanorods $|L(\omega_1)^2 L(\omega_2)^2|$ fail to account for the observed decrease in the emission of gold nanorods at higher aspect ratios, and the theory vastly overestimates the emission wavelength maximum for rods of aspect ratio 6.0 predicted at 970 nm. Thus, the intrinsic luminescence of bulk gold must be incorporated into this model, or β_1 should be incorporated. A theory has been proposed by Apell[32] describing the fluorescence emission as a coupling between the optical properties of gold and the transitions of its d-electrons. This theory predicts that the when the plasmon resonance is around the d-orbital transitions the emission is enhanced. The differential luminescence scattering power as a function of the emitted and scattered photons, $d^2P^0/d\Omega\, d\omega_2$, was modeled using the equation

$$\frac{d^2P^0}{d\Omega\, d\omega_2} \cong \frac{\omega_2}{\alpha(\omega_1) + \alpha(\omega_2)} \frac{|t_2|^2}{n_2^2 + k_2^2} D_2^0(\omega_2) \qquad (5)$$

with

$$D_2^0 \approx \int_{E_F - \omega_1}^{E_F - \omega_2} dE[\zeta_d^<(E)]^2 \qquad (6)$$

where $\zeta_d^<$ is the density of states of the filled d-orbitals[36] fitted by Origin, n and k are from Johnson and Christy,[35] the transmission factor is for light with polarization perpendicular to the surface, and $\alpha(\omega)$ is the absorption at the exciting and emission wavelength. This theory leads to the interpretation that the observed enhanced emission arises from the d-orbital transitions and the reflection and absorption constants of gold. These results are compared to the fluorescence emission determined by Mooradian[3] as shown in Figure 5. It should be noted that this theory overestimates the emission above 700 nm, and as a result it is not a good equation to use to determine the corrected emission. Thus, the experimental results of Moordian[3] were tabulated and used as β_1 in eq 3 to calculate the emission spectra. To compare the calculated spectra with the observed ones, self-absorption has to be taken into account. The self-absorption of the nanorod emission due to absorption by the plasmon resonance absorption before reaching the detector is taken into account by subtracting the experimental absorption spectrum (which includes the transverse and longitudinal plasmon resonance) from the calculated emission spectrum. The experimental absorption spectrum was multiplied by 10,000,000 to account for the differences between theoretical calculations and experimental intensities. Since we are interested in band shapes, the absolute intensities are not important; in fact, their units are different.

Discussion

The calculated fluorescence emission spectra presented in Figure 4b is a compilation of the calculated enhancement factor from eq 3 by Boyd and Shen[24−26] using 470-nm excitation, aspect ratio distribution results from the fit of the calculated spectra using eq 4 by Gans[33] to the observed absorption spectrum, the observed emission of bulk gold from Mooradian,[3] and the self-absorption correction using the observed absorption

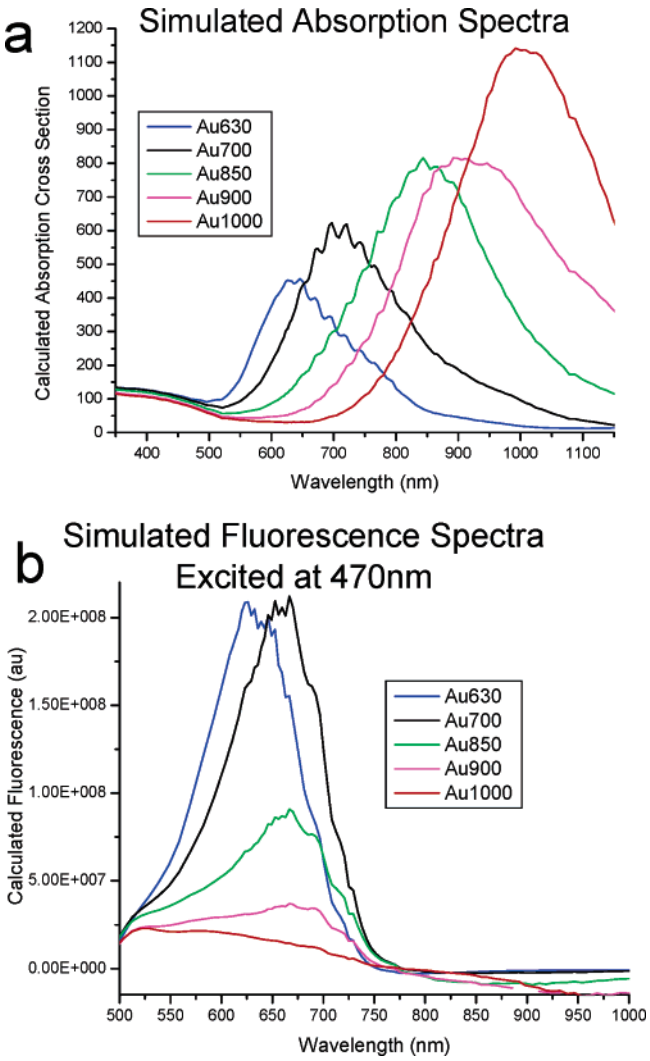

Figure 4. (a) Calculated absorption spectra of samples fit to experimental data in Figure 2a by adjusting the aspect ratio distribution. (b) Calculated emission spectra of nanorod samples excited at 470 nm. (See text for method of calculation.)

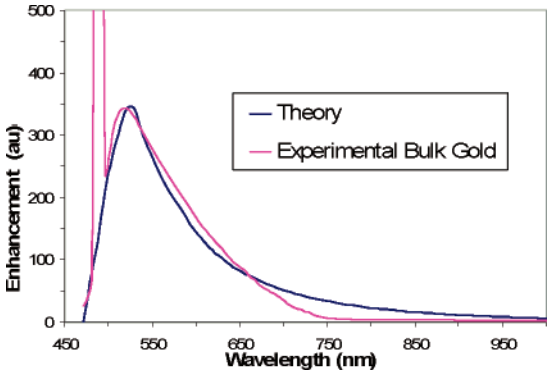

Figure 5. Emission spectra of bulk gold from Mooradian experimental data and Apell's theory. See text for equations.

spectra. These results are then compared to the experimental results in Figure 2b and in Table 1. Using the absorption spectra as a model for the aspect ratio distribution generates reasonable agreement with experimentally observed emission, especially after self-absorption has been corrected. Both absorption and emission examine a macroscopic volume of the sample in solution and generate an averaged signal across the sample. The emission spectra calculated in Figure 4b resemble the observed emission in Figure 2b in shape and shifting emission wavelength.

TABLE 1: Experimental and Theoretical Values Obtained for the Different Samples Studied[a]

	experimental samples				theory			
sample	plasmon max(nm)	emission max (nm)	emission intensity (au)	emission intensity (norm)	aspect ratio	emission max (nm)	emission intensity (au)	emission intensity (norm)
Au630	630	572	1302	1.00	2.25	635	2.09×10^8	1.00
Au700	705	597	989	0.76	3.25	660	2.10×10^8	1.00
Au850	845	598	681	0.52	4.75	667	9.09×10^7	0.43
Au900	900	615	649	0.50	5.00	673	3.70×10^7	0.18
Au1000	995	603	507	0.39	6.00		2.14×10^7	0.10

[a] The experimental position of the longitudinal plasmon resonance, emission wavelength, and emission maximum for gold nanorods obtained in the present study are presented in addition to the values obtained theoretically, the aspect ratio, the emission wavelength, and emission intensity.

The calculated values of the emission wavelength maxima obtained theoretically are slightly red-shifted from those observed experimentally, but this difference is much less than that presented by Mohamed et al.[17] due to the incorporation of the fluorescence spectra of bulk gold in the present treatment. (For an aspect ratio of 5.4, their calculated emission maximum is 725 nm compared to 588 nm for their observed maximum.[17]) The decrease in the intensity is due to the decrease in the emission of bulk gold as the wavelength of light increase is related to the density of states of the d-orbitals in gold. The emission of Au630 is theoretically predicted to be of the same intensity as the emission of Au700, but experimentally the intensity of Au700 is found to decrease. This difference could be due to the higher percentage of spheres in Au700 as observed by the larger absorption at 520 nm and their contribution to the absorption of the excitation light (at 480 nm). This difference could also be due to the difference in the nonradiative rates of the different samples, generating lower intensity as the aspect ratio is increased. Samples Au630 and Au700 are observed to fluoresce at their minimum absorption as observed in Figures 2a and 2b, generating the larger observed emission intensities. Erroneous results are obtained before self-absorption is taken into account. The emissions for samples Au850, Au900, and Au1000 are predicted to be above 750 nm, but the plasmon resonance becomes more intense at higher aspect ratios, and the emission of bulk gold decreases at 700 nm, leading to the observed emission cutoff at ~750 nm.

The detector used for this experiment does not have sensitivity above 800 nm, but by observation of the calculated emission spectra in Figure 4b, the gold is predicted to have much less emission above this wavelength due to the limitation of the spectral width of the emission spectrum of the bulk metal. It is important to take into account the emission of bulk gold in the equation when larger aspect ratios are used due to the limited emission from bulk gold at higher wavelengths. It is also important to notice that the theory for predicting bulk gold emission also overestimates the emission at longer wavelengths. Thus, the theory presented here is able to predict the observed results, where the emission wavelength stops shifting for higher aspect ratio nanorods due to the limits imposed by the emission spectrum of bulk gold. These results can be interpreted using the theoretical models presented here to show that as the aspect ratio increases and as the longitudinal plasmon resonance absorption shifts away from the interband transition (as reflected by the fluorescence of the bulk gold), the enhancement decreases. This shows that as the aspect ratio continues to increase, the enhancement does not continue to increase as suggested by previous results.

The results suggest that interband enhanced fluorescence from gold nanorods will be limited to those with aspect ratios for which the longitudinal surface plasmon absorption band is overlapping with the interband absorption and fluorescence bands. The previously determined quantum yield by Mohamed et al.[17] for these rods and its increase with aspect ratio in the spectral region of overlap are due to the increase in the absorption cross section of the surface plasmon absorption and the larger overlap of the bands of the bulk metal as the aspect ratio increases. In that case, the overlap between the interband absorption and the surface plasmon absorption increases as the aspect ratio increases and the fluoresce emission enhancement increases, leading to the predicted and observed increase in the quantum yield by Mohamed et al.[17] Within the broad interband absorption, as the aspect ratio increases, the surface plasmon absorption band shifts to a longer wavelength, which causes the enhanced fluorescence spectrum maximum to shift to a longer wavelength, as shown and predicted in the previous studies. As the surface plasmon absorption overlaps with the emission spectral wavelength region, the amount of the overlap becomes important in determining the emission enhancement. In the current study, the longitudinal surface plasmon absorption band moves to a longer wavelength than the bulk fluorescence spectrum by increasing the aspect ratio, leading to a decrease in the enhancement, as predicted and observed. Table 1 shows that as the aspect ratio increases from 2.25 to 6.0 the predicted intensity of the enhanced fluorescence decreases by an order of magnitude. The observed intensity, however, decreases by only a factor of 2.5. The more sluggish sensitivity of the observed emission intensity to the aspect ratio (compared to the predicted change in the radiative cross section) supports the fact that the nonradiative relaxation process of the excited interband excited state is very rapid. To detect emission, the enhanced emission has to be of sufficient cross section to compete with the rapid nonradiative processes. In spheres, the surface plasmon absorption cross section is much smaller than the longitudinal absorption band in the rods. For this reason, no enhanced fluorescence is observed from spheres. One also expects fluorescence could be quenched for very high aspect ratio nanorods where the overlap between the longitudinal band and the interband transition is not very good or for which the adsorbed capping material increases the nonradiative relaxation probability.

Comments on the 740-nm Emission

An emission was observed at ~740 nm in all of the rods as well as the spheres with different surfactants, which suggests it is a property of the metal nanoparticles. Thus, this emission is not specific to the shape in contrast to the other emission around 600 nm, which is observed to be enhanced for nanorods specifically. The 740-nm emission was not observed for solutions not containing gold nanoparticles. The theory presented in this paper predicts that emission at 740 nm corresponds to an aspect ratio of 3.75, which is unlikely to be present in a sample of spheres; thus this emission is not attributed to shape-

TABLE 2: Absorption and Fluorescence Emission at 740 nm

	absorbance: theory		fluorescence: experiment	
sample	intensity at 740 nm (au)	normalized	intensity at 740 nm (au)	intensity corrected[a] (au)
Au630	245	2.6	686	1788
Au700	564	6.0	376	2262
Au850	453	4.8	380	1833
Au900	245	2.6	601	1566
Au1000	93.8	1.0	460	460

[a] The experimental fluorescence is corrected for self-absorption.

enhanced emission. In Figure 4b, the emission spectra calculated displays a decrease almost to the baseline by 750 nm, due to the decrease in the emission of bulk gold in the near-IR, and does not predict a separate emission at 740 nm as was observed experimentally.

To gain more insight into the origin of this near-IR emission, we tried to examine its intensity dependence on the aspect ratio. To determine accurate relative intensities, the self-absorptions of the different samples are corrected and given in Table 2. The experimentally observed emission intensity and the theoretically calculated absorption cross section at 740 nm are presented. The absorption cross section is normalized to the minimum value of 1. Then the experimentally observed emission intensity is multiplied by the absorption cross-section normalization to obtain the corrected relative emission intensity. This shows that the emission observed is enhanced by the surface plasmon resonance or the largest absorption cross section at 740 nm leads to the largest emission intensity, after self-absorption has been taken into account. Thus, the sample with the plasmon resonance furthest from 740 nm, Au1000, has the least emission intensity after self-absorption correction. Samples that have the same absorption cross section have similar emissions, even though the maximum plasmon resonance absorptions are on opposite energy sides of the emission. Thus, explanations of the origin of this emission should include the sensitivity of the absorption of the sample due to the plasmon resonance as a mechanism to enhance the near-IR emission.

Several proposed sources of this emission were given previously. A similar emission is observed by Jian et al.,[37] attributed to aggregate emission. Beversluis et al.[38] also observe a separate emission in the IR that increases around 720 nm, which displays different dependences, and cannot be explained by the same mechanism as the visible emission. Au_{23} has been shown to have an emission around this wavelength,[9] so it is possible that this emission is due to small clusters present in solution. Reports suggest that the band edge of gold is around 1.7 eV (730 nm).[32,39] This would suggest that the emission observed at 740 nm could be band-edge emission due to the recombination of electrons enhanced by the surface plasmon transition. This emission could also be the background emission present in SERS spectra.[18−23] The background spectrum is only observed with the SERS signal when both the rough metal surface and the molecule are in contact[18,19] and is believed to be due to a metal−molecule charge-transfer interaction.[20−23] This background emission was previously observed to be independent of size and shape of the nanoparticle[40] but related to both the metal and the adsorbed molecule. Thus, the emission at 740 nm could be due to a state created by adsorption of a molecule on the surfaces of the nanorods (or nanospheres).

Acknowledgment. We acknowledge Dr. Stephan Link and Dr. Robert Whetten for stimulating discussion and suggestions and the financial support of the National Science Foundation, Division of Material Science, Grant No. 0138391.

References and Notes

(1) Link, S.; El-Sayed, M. A. *Int. Rev. Phys. Chem.* **2000**, *19*, 409.
(2) Kamat, P. V. *J. Phys. Chem. B* **2002**, *106*, 7729.
(3) Mooradian, A. *Phys. Rev. Lett.* **1969**, *22*, 185.
(4) Wilcoxon, J. P.; Martin, J. E.; Parsapour, F.; Wiedenman, B.; Kelley, D. F. *J. Chem. Phys.* **1998**, *108*, 9137.
(5) Hwang, Y. N.; Jeong, D. H.; Shin, H. J.; Kim, D.; Jeoung, S. C.; Han, S. H.; Lee, J. S.; Cho, G. *J. Phys. Chem. B* **2002**, *106*, 7581.
(6) Huang, T.; Murray, R. W. *J. Phys. Chem. B* **2001**, *105*, 12498.
(7) Link, S.; Beeby, A.; FitzGerald, S.; El-Sayed, M. A.; Schaaff, T. G.; Whetten, R. L. *J. Phys. Chem. B* **2002**, *106*, 3410.
(8) Zheng, J.; Petty, J. T.; Dickson, R. M. *J. Am. Chem. Soc.* **2003**, *125*, 7780.
(9) Zheng, J.; Zhang, C.; Dickson, R. M. *Phys. Rev. Lett.* **2004**, *93*, 077402.
(10) Bruzzone, S.; Arrighini, G. P.; Guidotti, C. *Chem. Phys.* **2003**, *291*, 125.
(11) Geddes, C. D.; Parfenov, A.; Gryczynski, I.; Lakowicz, J. R. *Chem. Phys. Lett.* **2003**, *380*, 269.
(12) Jian, Z.; Yongchang, W.; Qin, W. *Acta Photonica Sin.* **2003**, *32*, 357.
(13) Maali, A.; Cardinal, T.; Treguer-Delapierre, M. *Physica E* **2003**, *17*, 559.
(14) Varnavski, O. P.; Mohamed, M. B.; El-Sayed, M. A.; Goodson, T., III. *J. Phys. Chem. B* **2003**, *107*, 3101.
(15) Wang, G.; Huang, T.; Murray, R. W.; Menard, L.; Nuzzo, R. G. *J. Am. Chem. Soc.* **2005**, *127*, 812.
(16) Geddes, C. D.; Parfenov, A.; Gryczynski, I.; Lakowicz, J. R. *J. Phys. Chem. B* **2003**, *107*, 9989.
(17) Mohamed, M. B.; Volkov, V.; Link, S.; El-Sayed, M. A. *Chem. Phys. Lett.* **2000**, *317*, 517.
(18) Jiang, J.; Bosnick, K.; Maillard, M.; Brus, L. *J. Phys. Chem. B* **2003**, *107*, 9964.
(19) Michaels, A. M.; Nirmal, M.; Brus, L. *J. Am. Chem. Soc.* **1999**, *121*, 9932.
(20) Persson, B. N. J.; Baratoff, A. *Phys. Rev. Lett.* **1992**, *68*, 3224.
(21) Birke, R. L.; Lombardi, J. R.; Gersten, J. I. *Phys. Rev. Lett.* **1979**, *43*, 71.
(22) Lombardi, J. R.; Birke, R. L.; Lu, T.; Xu, J. *J. Chem. Phys.* **1986**, *84*, 4171.
(23) Adrian, F. J. *J. Chem. Phys.* **1982**, *77*, 5302.
(24) Boyd, G. T.; Yu, Z. H.; Shen, Y. R. *Phys. Rev. B* **1986**, *33*, 7923.
(25) Boyd, G. T.; Rasing, T.; Leite, J. R. R.; Shen, Y. R. *Phys. Rev. B* **1984**, *30*, 519.
(26) Chen, C. K.; Heinz, T. F.; Ricard, D.; Shen, Y. R. *Phys. Rev. B* **1983**, *27*, 1965.
(27) Otto, A.; Mrozek, I.; Grabhorn, H.; Akemann, W. *J. Phys.: Condens. Matter* **1992**, *4*, 1143.
(28) Nikoobakht, B.; El-Sayed, M. A. *Chem. Mater.* **2003**, *15*, 1957.
(29) Link, S.; Mohamed, M. B.; El-Sayed, M. A. *J. Phys. Chem. B* **1999**, *103*, 3073.
(30) Yan, B.; Yang, Y.; Wang, Y. *J. Phys. Chem. B* **2003**, *107*, 9159.
(31) Link, S.; El-Sayed, M. A. *J. Phys. Chem. B* **2005**, *109*, 10531.
(32) Apell, P.; Monreal, R.; Lundqvist, S. *Phys. Scr.* **1988**, *38*, 174.
(33) Gans, R. v. *Ann. Phys.* **1915**, *47*, 270.
(34) Mie, G. *Ann. Phys.* **1908**, *25*, 377.
(35) Johnson, P. B.; Christy, R. W. *Phys. Rev. B* **1972**, *6*, 4370.
(36) Kupratakuln, S. *J. Phys. C: Solid State Phys.* **1970**, *3*, S109.
(37) Jian, Z.; Liqing, H.; Yongchang, W.; Yimin, L. *Physica E* **2004**, *25*, 114.
(38) Beversluis, M. R.; Bouhelier, A.; Novotny, L. *Phys. Rev. B* **2003**, *68*, 115433.
(39) Alvarez, M. M.; Khoury, J. T.; Schaaff, G.; Shafigullin, M. N.; Vezmar, I.; Whetten, R. L. *J. Phys. Chem. B* **1997**, *101*, 3706.
(40) Nikoobakht, B. Synthesis, Characterization and Self-Assembly of Gold Nanorods and Surface-Enhanced Raman Studies. Ph.D. Thesis, Georgia Institute of Technology, 2003.